2006

Design of near-optimal waveforms for chest and abdominal compression and decompression in CPR using computer-simulated evolution

Charles F. Babbs
Purdue University, babbs@purdue.edu

Design of near-optimal waveforms for chest and abdominal compression and decompression in CPR using computer-simulated evolution

Charles F. Babbs

Department of Basic Medical Sciences and Weldon School of Biomedical Engineering, Purdue University; 1246 Lynn Hall, West Lafayette, IN 47907, USA

(Resuscitation, 68, 277-293, 2006)

Abstract

Objective: To discover design principles underlying the optimal waveforms for external chest and abdominal compression and decompression during cardiac arrest and CPR.
Method: A 14-compartment mathematical model of the human cardiopulmonary system is used to test successive generations of randomly mutated external compression waveforms during cardiac arrest and resuscitation. Mutated waveforms that produced superior mean perfusion pressure became parents for the next generation. Selection was based upon either systemic perfusion pressure (SPP=thoracic aortic minus right atrial pressure) or upon coronary perfusion pressure (CPP=thoracic aortic pressure minus myocardial wall pressure). After simulations of 64,414 individual CPR episodes, 40 highly evolved waveforms were characterized in terms of frequency, duty cycle, and phase. A simple, practical compression technique was then designed by combining evolved features and a constant rate of 80/min and duty cycle of 50%.
Results: All ultimate surviving waveforms included reciprocal compression and decompression of the chest and the abdomen to the maximum allowable extent. The evolved waveforms produced 1.5 to 3 times the mean perfusion pressure of standard CPR and greater perfusion pressure than other forms of modified CPR reported heretofore, including ACD+ITV and IAC-CPR. When SPP was maximized by evolution, the chest compression/abdominal decompression phase was near 70% of cycle time. When CPP was maximized, the abdominal compression/chest decompression phase was near 30% of cycle time. Near-maximal SPP/CPP of 60/21 mmHg (forward flow 3.8 L/min) occurred at a compromise compression frequency of 80/min and duty cycle for chest compression of 50%.
Conclusions: Optimized waveforms for thoraco-abdominal compression and decompression include previously discovered features of active decompression and interposed abdominal compression. These waveforms can be utilized by manual (Lifestick-like) and mechanical (vest-like) devices to achieve short periods of near normal blood perfusion noninvasively during cardiac arrest.

Key words: ACD-CPR, Cardiopulmonary resuscitation (CPR); Coronary perfusion pressure; Device; IAC-CPR, Mathematical model, Vest CPR

---

1. Introduction

Those of us who study CPR hemodynamics believe that how you push and how you blow can make a difference in the outcome of resuscitation from cardiac arrest. There is evidence that this belief, first articulated to the author by Peter Safar, is true. Clinical trials of interposed abdominal compression CPR by Sack and coworkers[1] showed double the probability of immediate survival, 24-hour survival, and discharge survival using a technique shown in the laboratory to produce about twice the blood flow of standard CPR[2,3]. Recently, Aufderheide, Lurie, and coworkers showed similar effects using an impedance threshold valve attached to the airway during otherwise standard CPR to augment negative pressures in the chest between compressions[4-6]. Thus it seems that despite the myriad of intervening events that happen to patients between restoration of spontaneous circulation and hospital discharge, improved perfusion for just a few short minutes during CPR itself can have a major influence upon long-term outcome.

The question therefore arises as to what is the optimal way to generate an artificial circulation through manipulation of external pressures on the body. A large literature points to the potential of a combination, whenever feasible, of abdominal and chest compressions[3,7] and also to a combination of both compression and decompression (with the aid of an only slightly modified plumber's plunger for the chest, or an adhesive pad for the abdomen)[8,9]. That is to say, optimal CPR is likely to have 4 phases—including compression and decompression of both the chest and the abdomen. Such maneuvers are possible either with vest-like automatic machines[10] or with a Lifestick® - like device in the hands of a single rescuer[11]. The identification of 4 phases, however, still leaves a feature space filled with many of possible waveforms for applied force and/or applied pressure. How can CPR machines best be programmed? What is the optimal technique for ordinary human rescuers?

The present paper describes a new intellectual strategy for optimizing CPR using simulated evolution in a computer model of the cardiopulmonary system that incorporates airways, lungs and 14 vascular compartments. This model allows the performance of thousands of thought experiments with randomly mutated compression waveforms to conduct a guided search for optimal waveforms in a multidimensional feature space. The results suggest that standard CPR is far from optimal and that pressures and flows approaching normal resting levels can be achieved. The price of high blood flow, however, is high pulmonary vascular pressure, which can only be sustained for a few minutes without creating pulmonary edema. Fortunately, only a few minutes of effective CPR may be needed.

2. Methods

2.1 Approach to simulated evolution

Simulated evolution is a simple, robust, and popular way to solve optimization problems that can be modeled on a computer[12-15]. At its core, the natural evolution of genes is the repeated combination of random variation and nonrandom selection. This sequence is at the heart of

evolution in bacteria that do not have routine sexual recombination of genes. (Although some simulated evolution schemes include recombination of surviving genes, sex is not necessary for evolution.) In the problem at hand the "gene" is the set of instructions for making a chest or abdominal compression waveform in CPR, that is, a function describing the amount of external compression or decompression that is applied over time. The evolving organisms are the computer models that implement the waveform specifications. The phenotype is the artificial circulation produced by the each model. The fitness of the organism for survival is the mean perfusion pressure. The non-random selection is done to maximize either mean systemic or mean coronary perfusion pressure.

Computer models of the circulation in cardiac arrest and CPR are now rather well developed[16-18] and can be readily adapted for simulated evolution. Realistic constraints on the problem make it even easier. For example, a safe maximal chest compression force of 400 Newtons for adults can be assumed. The maximal possible decompression pressure in the chest is about –20 mmHg[19,20]. Here we specify a chest compression waveform as a dimensionless function of time ranging somewhere between –0.2 and +1.0. The actual value of chest force is the product of the chest waveform function and a constant, Fmax-chest = 400 N. Similarly the actual value of pressure on the abdomen is the product of the abdominal waveform function and a constant, Pmax-abd = 100 mmHg. With these constraints chest force can range anywhere from –80 Newtons to +400 Newtons. The external abdominal pressure can range anywhere from –20 mmHg to +100 mmHg.

Another reasonable constraint on the optimal waveform is that it should be periodic. That is, the pattern of compression in time should be a repeated sequence that is not too long for rescuers to remember. Here we choose a 3 second interval as the basic period, so that the final result must repeat itself in at most every 3 seconds. Within this 3-second interval a pattern of compression may well repeat more frequently if it is beneficial to the circulation of blood. To simplify the problem further, we divide the fundamental 3 sec period into 24 discrete segments, each 1/8 sec in duration, and 13 discrete levels of amplitude from –0.2 to +1.0, in increments of 0.1. Within this framework the chest compression force can be specified in terms of 24 numbers, each ranging from 1.0 x 400 = 400 N to –0.2 x 400 = -80 N, representing the force applied in successive 1/8 sec intervals. Similarly, the abdominal compression pressure can be specified in terms of 24 numbers, ranging from 1.0 x 100 = 100 mmHg to –0.2 x 100 = -20 mmHg. The two "genes" for chest and abdominal compression waveforms, therefore, consist together of 48 units or loci, each of which can take on 13 possible values. These possible compression values could be represented by one of the letters A—M in a way similar to the alphabet of nucleotide bases (A, C, G, T) in biological genes. For example, one could denote a CPR waveform gene as "start-ABCFGHLM …. LHCBA-finish" just as one could denote a bacterial gene as 3'-AGTCCTG ….GCCTAGGA-5'. In addition, one could specify two "master genes" for Fmax-chest and Pmax-abd, which control the expression of the chest and abdominal waveform genes. In this paper, however, we shall leave the master genes fixed and focus on the waveform genes.

The mutation-selection mechanism works on one individual locus at a time and creates one offspring per generation. Survival of a set of waveform genes is based upon superior systemic perfusion pressure (SPP) or coronary perfusion pressure (CPP), as explained in detail subsequently. The steps of simulated evolution of mean perfusion pressure, $\overline{P}$, are as follows:

1. Begin with a random waveform, W,
2. Run the model to get $\overline{P}(W)$
3. Randomly mutate W to get a mutant or modified waveform, M
4. Run the model to get $\overline{P}(M)$
5. If $\overline{P}(M) > \overline{P}(W)$, set W = M
6. Go to step 2

This sequence is repeated many hundreds of times or until W is stable. In the present study we ran the circulation model for 27 sec intervals and calculated average perfusion pressure over the last 6 seconds from 21 to 27 seconds as a figure of merit or "fitness" for a particular set of chest and abdominal waveform genes. The range from 21 to 27 sec represented steady-state pressures between ventilations. Ventilatory pauses and compression/ventilation ratios were not modeled in this initial study.

2.2. Simulated evolution strategy

The goal is to find near-optimal practical waveforms, which are relatively simple to learn or to implement mechanically, and which are devoid of useless appendages and idiosyncrasies that can crop up in evolved forms. Hence we are not interested so much in particular winning designs, but rather in winning design concepts or principles. These are embodied in the statistical properties of the waveforms, including frequency, duty cycle, range, and thoraco-abdominal phasing. Hence our strategy is to create a number of highly evolved, successful waveforms that produce large perfusion pressures and then to characterize their statistical properties. It is quite reasonable to include human intervention at this point, because our objective is to find highly effective waveforms not to create a computer program to find such waveforms automatically. In this way we can clean up the evolved forms to create a simple hybrid waveform with similar statistical properties. This last step is similar in effect to breeding desirable organisms with one another to combine their best traits.

In implementing this strategy it is important to start with random seed genes initially to avoid the problem of premature convergence to a local optimum. As shown in Figure 1, simple mutation-selection algorithms tend to produce "hill climbing" in the search space. This process is akin to the behavior of hikers who begin at an arbitrary point in a mountain range and always walk up hill. They will find the nearest peak, but will not necessarily find the highest peak in the mountain range. However, if one tracks many individual hill climbers from multiple random starting points, the probability of finding the highest peak increases. (That is, include both path oriented and volume oriented search techniques[12].) The number of random starting points required depends on the complexity of the terrain. In general, one cannot be guaranteed of finding the exact maximum. One may find K2 rather than Everest in the Himalayas. However, if we are satisfied with finding new, highly effective waveforms, if not the absolute best, or if the terrain in the search space is not too complex, then this strategy is simple and effective. Moreover, finding sharp, narrow peaks would be impractical, because moving a short distance away from the summit would produce a large fall-off in performance. What we really want to find is the highest broad peak in the range.

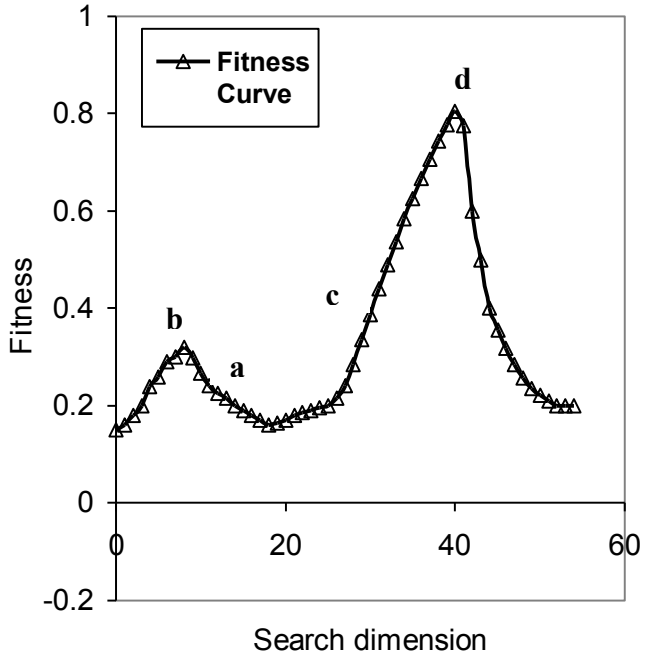

Figure 1. A one-dimensional slice through a multi-dimensional search space. A hiker randomly placed at "a" who gradually walks uphill will wind up at secondary peak "b". Another hiker randomly placed at "c" will find higher peak "d". The hiker who started at "a" is trapped at a secondary peak.

2.3. Mutation and selection

Here mutation is defined as a ± 0.1 unit change in either chest or abdominal waveform amplitude within the prescribed range of –0.2 to 1.0. This step size is very close to the theoretical step size for optimal convergence rate for our problem, namely, 0.09, described by Back and Schwefel[12]. In some trials of evolution two or three such mutations were made for the first several hundred generations, as advocated by Fogel[15], to speed convergence and avoid stagnation. However, this strategy did not improve perfusion pressures. Evolution was continued for a maximum of 2000 generations or until a single gene survived for 200 generations without being replaced by a superior sequence. Original starting positions were obtained by random assignment of values at all 48 loci over using a uniform distribution. This entire process was repeated to generate 40 highly evolved survivors, each starting from a different random seed—half using SPP as the fitness criterion and half using CPP, as described in section 2.5.

2.4. Numerical methods

2.4.1. Computational model of the circulation

The computational model of the circulation is described in detail in Appendix 1 and in reference[21]. In brief, the model used (Figures 2 and 3) is an adaptation of that previously published for resuscitation research by this author[18]. The number of vascular compartments is increased from 7 to 14 in order to include explicitly the anatomic details of the pulmonary circulation and a 4-chambered heart (Figure 3). The model is based upon normal human anatomy and physiology, the definition of compliance (volume change / pressure change), and Ohm's Law (flow = pressure / resistance). The human circulatory system is represented by 14 compliant chambers, connected by resistances through which blood may flow, as shown in Figures 2 and 3. Definitions of the subscripts indicating particular vascular structures are provided in Table 1. The compliances correspond to the thoracic aorta, abdominal aorta, carotid arteries, femoral arteries, jugular veins, leg veins, right atrium and superior vena cava, right ventricle, central pulmonary arteries, peripheral pulmonary arteries, left atrium and central pulmonary veins, peripheral pulmonary veins, and left ventricle.

Table 1: Nomenclature

Symbol	Definition
Subscripts	
aa	Abdominal aorta
a	Aorta at level of diaphragm
ao	Thoracic aorta
av	Aortic valve
C, car	Carotid
cppa	Central to peripheral pulmonary arteries
cppv	Central to peripheral pulmonary veins
fa	Femoral artery
fv	Femoral vein
h	Head
ht	Heart
ia	Iliac artery
iv	Iliac vein
ivc	Inferior vena cava
j, jug	Jugular
L	Lungs
l	Legs
la	Left atrium and central pulmonary veins
lv	Left ventricle
M	Mediastinum
mv	Mitral valve
pa	Pulmonary arteries (central)

pc	Pulmonary capillaries
ppa	Peripheral pulmonary arteries
ppv	Peripheral pulmonary veins
pv	Pulmonic valve
ra	Right atrium and superior vena cava
s	Systemic circulation below diaphragm
tv	Tricuspid valve
v	Portal and systemic veins at level of diaphragm

Variables

A	Cross sectional area (cm^2)
C	Compliance (L/mmHg or ml/mmHg)
d_0	Resting front to back dimension of mediastinal soft tissues (cm)
E	Young's modulus of elasticity (Pa or mmHg)
$F(t)$	External force applied to chest over time
f_{tp}	Thoracic pump factor (0 – 1)
i	Flow or current between compartments (L/sec or L/min)
k	Spring constant of chest (Nt/cm)
μ	Damping constant of chest (Nt/cm/sec)
P	Instantaneous pressure in a compartment (mmHg)
ΔP	Pressure increment during time Δt (mmHg)
R	Resistance (mmHg/(L/sec))
t	Time during a cycle of CPR (sec)
Δt	Time increment (sec)
V	Volume (ml)
x_0	Effective compression threshold (cm)
x_1	Sternal compression (cm)
$\dot{x}_1$	Rate of sternal compression (cm/sec)
x_2	Heart chamber expansion (cm)
$\dot{x}_2$	Rate of heart chamber expansion (cm/sec)

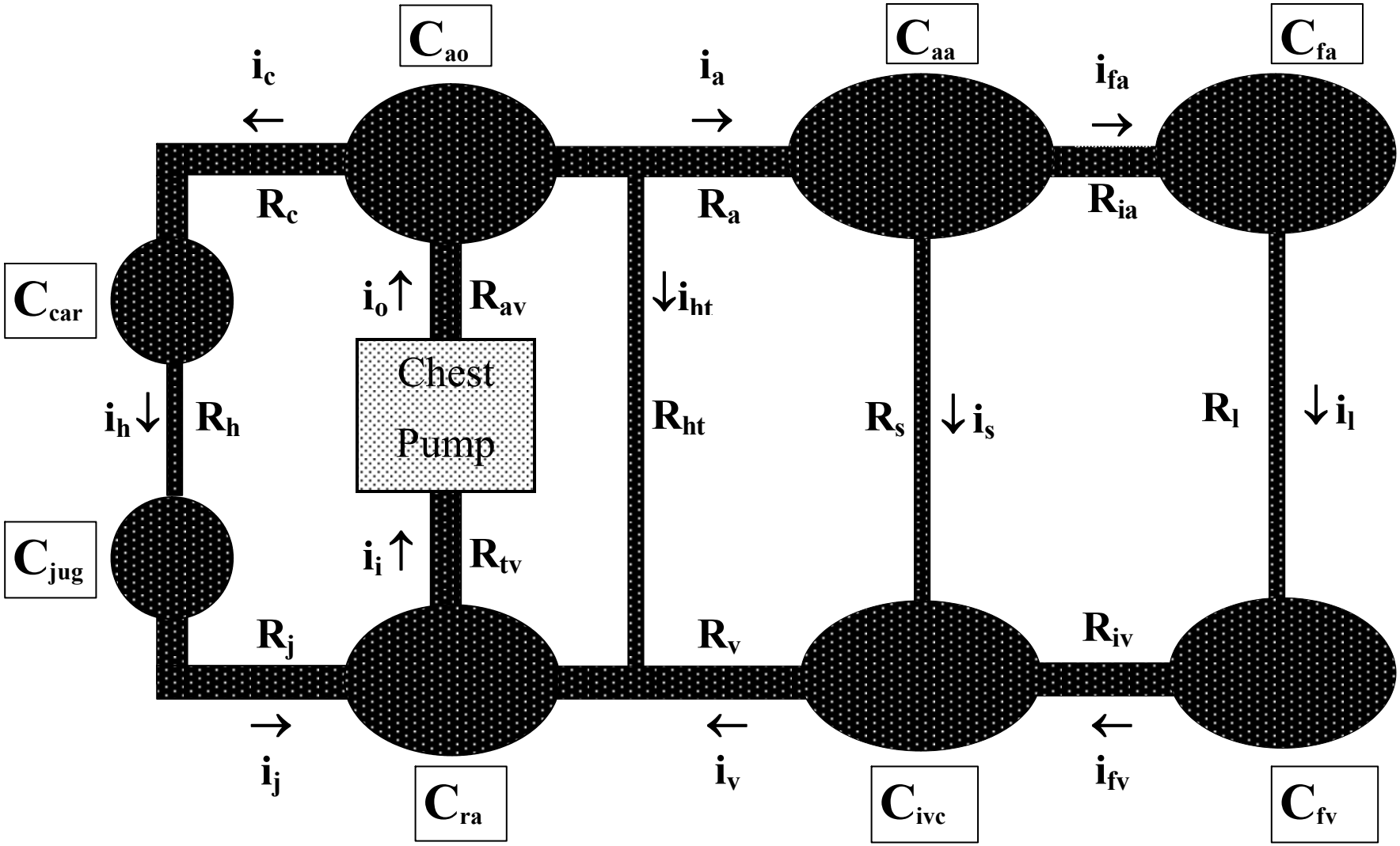

Figure 2. Model of the human circulatory system.

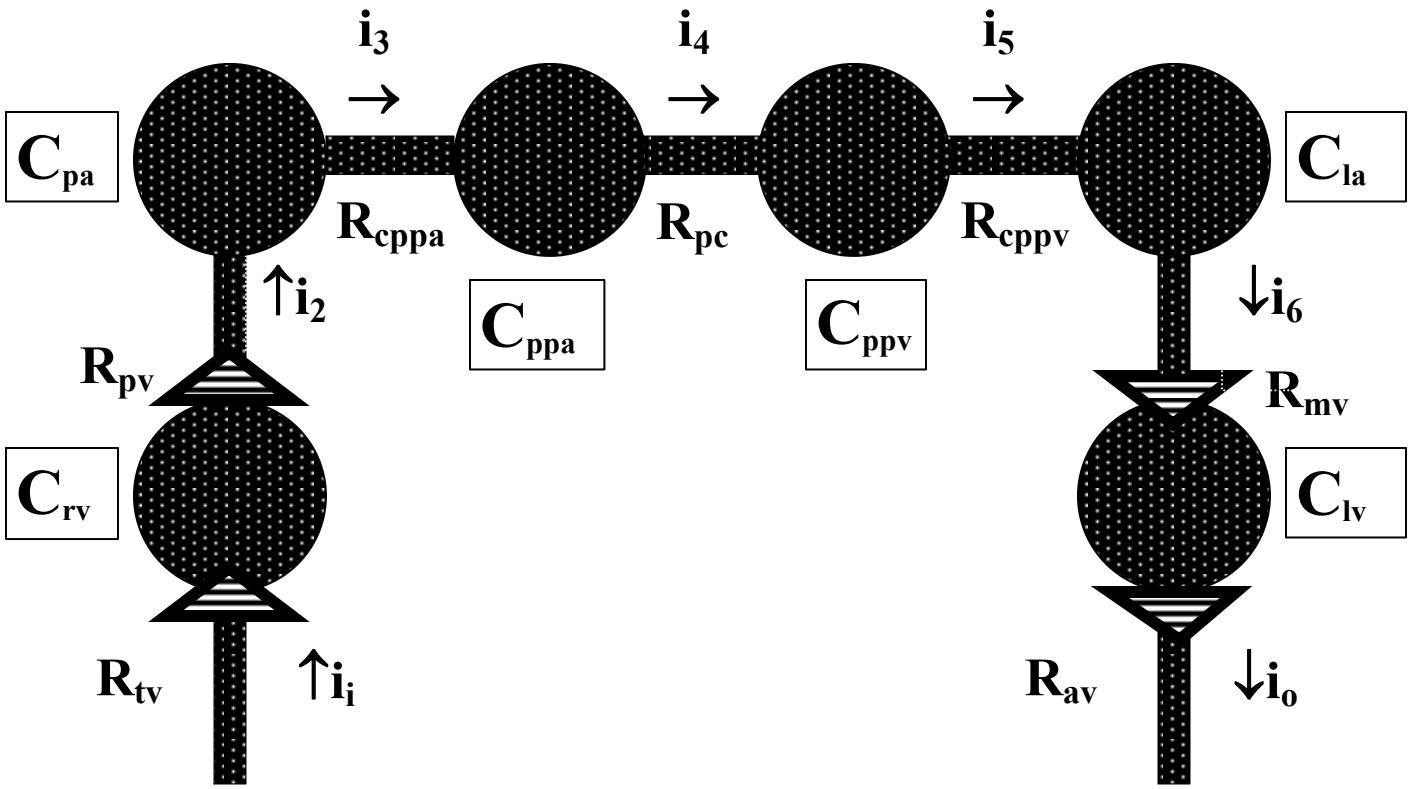

Figure 3. Detailed components within the chest. Triangles indicate heart valves.

Conductance pathways with non-zero resistances, R, connect the vascular compartments. The values of R_h, R_{ht}, R_s and R_l are large and represent resistances of the systemic vascular beds of the head, heart, trunk, and legs. R_c, R_a, R_j, R_{ia}, R_{iv}, R_{cppa} , R_{cppv} ,and R_v are small and represent in-line resistances of the great vessels. R_{pc} is intermediate in value and represents the resistance of the pulmonary capillary bed, which is much less than that of the systemic vascular bed. Also included are the small resistances, R_{tv}, R_{pv}, R_{mv}, R_{av}, which represent the inflow and outflow resistances of the tricuspid, pulmonic, mitral, and aortic valves of the heart. Niemann's valves between the chest and jugular veins at the level of the thoracic inlet are actual, but little known anatomic structures that function to block headward transmission of large positive pressure pulses in the chest during cough and also during CPR[22].

Chest wall. To model the influence of external chest compressions and lung ventilations upon the arrested circulation in CPR, the author adopted a simplified scheme illustrated in Figure 4, in which the opposition of the chest to external compression is represented as a simple spring and damper system. The figure is a diagrammatic cross section of the chest in prone position with sternum on the top and spine on the bottom. The whole chest and rib cage are regarded mechanically as paired springs and dampers with collective spring constant, k, and damping constant, μ. These resist a known time-varying external force, F(t), on the sternum. The depression of the sternum is denoted x_1. The chambers of the heart are supported and cushioned between the sternum and the spine by soft precardiac and retrocardiac soft tissues having Young's modulus of elasticity, E, and resting front-to-back dimension d_0.

Sternal motion. Motion of the sternum in response to force F(t) is given by the differential equation $F(t) - kx_1 - \mu\dot{x}_1 = 0$, for sternal displacement, x_1, and velocity of displacement $\dot{x}_1$. (Here the "dot" over x_1 indicates the first time derivative.) The constants k and μ are taken from the experimental results of Gruben et al[23] for the adult human chest. With the spring constant k = 75 Nt/cm and the damping constant μ = 2.75 Nt/cm/sec

Lungs. The lungs are regarded as gas filled balloons open to air via the tracheobronchial tree. For these compartments the pressure compared to atmospheric pressure is $P_{lung} = (\Delta V_{chest} + V_{in} - V_{out})/C_{lung}$, where ΔV_{chest} is the decrease in lung volume do to chest compression in CPR, $V_{in} - V_{out}$ is the net volume added via the airways, and C_{lung} is the combined lung-chest wall compliance. To model the functionality of an inspiratory impedance valve (for reference simulations of ACD-CPR) tracheal airflow was set to zero under the following conditions: ambient pressure = 0 and lung pressure < 0.

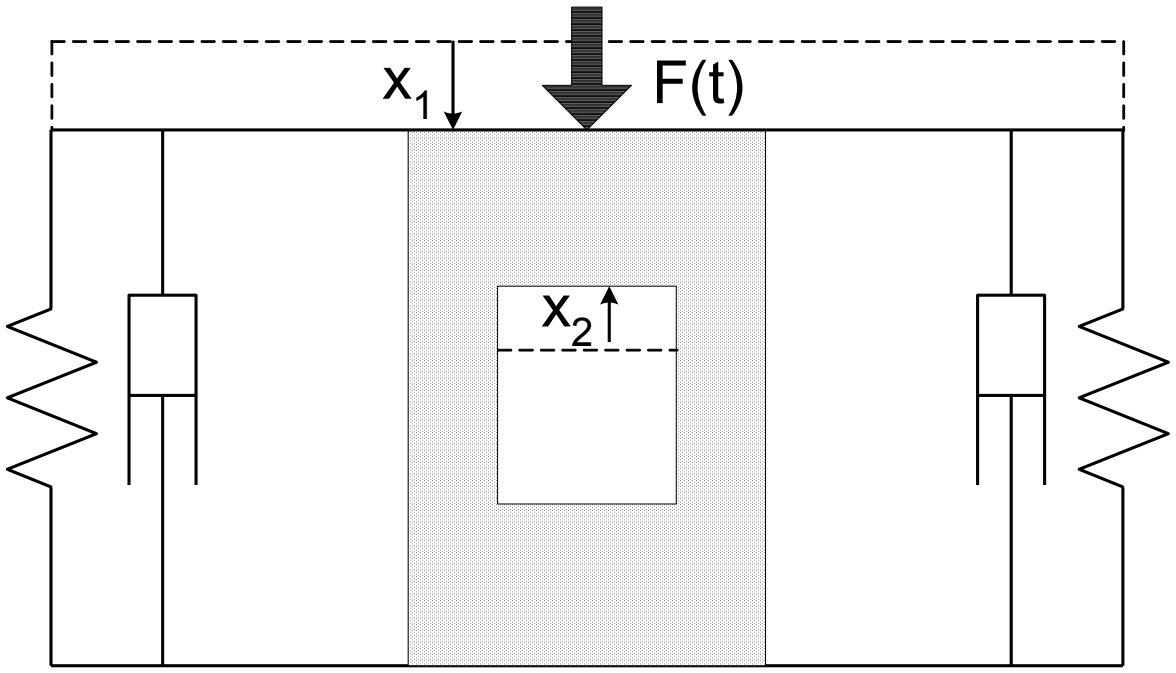

Figure 4: Model of chest wall, mediastinal tissues, and a representative cardiac chamber. The sketch represents a cross section of the chest; sternum on top. Outer springs and dampers represent the chest wall. F(t) is downward force applied to sternum. Outer springs and dampers represent the chest wall. x_1 represents compression of the sternum and anterior chest. x_2 represents expansion of the cardiac chamber with blood. Stippling represents mediastinal soft tissue having Young's modulus of elasticity, E.

Cardiac and thoracic pump mechanisms. In our model atria, central pulmonary arteries, central pulmonary veins, and thoracic aorta experience a combination of lung pressure and mediastinal pressure, P_M, according to the formula $P_{lung} + f_{tp} P_M$ for thoracic pump factor $0 \le f_{tp} \le 1$, depending on the degree to which the "thoracic pump" mechanism of CPR is working. When $f_{tp} = 1$ all mediastinal structures experience a uniform "global" intrathoracic pressure rise[24]. When $f_{tp} = 0$, only the right and left ventricular compliances are pressurized, as in open chest CPR[25-27]. Intermediate values of the thoracic pump factor allow models approximating the current understanding[28-30], in which for small animals and children blood is impelled predominantly by the cardiac pump mechanism (for example, $f_{tp} \approx 0.25$), whereas in larger animals and adult humans blood is impelled predominantly by the thoracic pump mechanism (for example, $f_{tp} \approx 0.75$). For simulated evolution we use the "adult" value of 0.75 exclusively.

2.4.2. Numerical integration

The model was solved using Microsoft Visual Basic to perform numerical integration of coupled differential equations describing incremental pressure changes in each vascular compartment. To model a cardiac arrest and CPR one begins with a uniform pressure such as 5 mmHg in all compartments of the arrested circulation and applies periodic waveforms of compression and decompression externally to the chest and abdomen. To model the normal circulation as a control, one applies pressures to the cardiac ventricles only. The incremental pressure changes in each vascular compartment are used to construct a marching solution for successive small increments of time, Δt, typically 0.001 sec. For simplicity and faster solutions of large numbers of models, the effective compression threshold defined in reference[31] was set to zero, so that mediastinal pressure became directly proportional to sternal deflection.

2.4.3. Model output

The output of the model is a multi-channel record of pressure as a function of time. Standard "normal" values of model parameters are given in Table 2 and in references[32,33]. Because of the high venous pressures and high myocardial tissue pressures that can occur during CPR, mean systemic perfusion pressure (thoracic aortic pressure minus right atrial pressure) or mean coronary perfusion pressure (thoracic aortic pressure minus left ventricular mural pressure) was used describe hemodynamic benefit[34]. These pressures were computed for the 21st through 27th seconds after onset of CPR to allow steady state conditions to develop.

Table 2: Model parameters

Resistances (>0)

	Value (mmHg/L/sec)	Definition
Rc	60	Resistance of both carotid arteries
Rh	5520	Resistance of the head vasculature
Rj	30	Resistance of both jugular veins
Rtv	5	Resistance of the tricuspid valve
Rpv	10	Resistance of the pulmonic valve
Rcppa	10	Resistance between central and peripheral pulmonary arteries
Rcppv	5	Resistance between central and peripheral pulmonary veins
Rmv	5	Resistance of the mitral valve
Rav	10	Resistance of the aortic valve
Rpc	105	Resistance of the pulmonary capillary bed
Rht	15780	Resistance of coronary vessels (heart)
Ra	25	Resistance of the aorta
Rv	25	Resistance of the inferior vena cava
Rs	1800	Resistance of residual systemic vasculature

Ria	360	Resistance of both iliac arteries
Riv	180	Resistance of both iliac veins
Rl	8520	Resistance of leg vasculature
Rairway	1.2	Resistance of airways to ventilation

Compliances (>0)

	Value (L/mmHg)	**Definition**
Crv	0.016	Compliance of the arrested right ventricle
Cpa	0.0042	Compliance of the large pulmonary arteries
Cppa	0.0042	Compliance of peripheral pulmonary arteries
Cppv	0.00128	Compliance of peripheral pulmonary veins
Cla	0.0128	Compliance of the left atrium and central pulmonary veins
Clv	0.008	Compliance of the arrested left ventricle
Ccar	0.0002	Compliance of both carotid arteries
Cjug	0.012	Compliance of both jugular veins
Cao	0.0008	Compliance of the thoracic aorta
Crh	0.0095	Compliance of the right atrium and intrathoracic great veins
Caa	0.0004	Compliance of the abdominal aorta
Civc	0.0234	Compliance of the inferior vena cava
Cfa	0.0002	Compliance of both femoral arteries
Cfv	0.0047	Compliance of both femoral veins

Other variables

	Value and units	**Definition**
A_L	100 cm^2	Cross section of lung squeezed by sternal compression
A_{ra} A_{la} A_{rv} A_{lv}	20 cm^2	Cross sectional area of cardiac chambers in front to back dimension--approximate
Frequency	80/min	Number of cycles per minute for chest and abdominal pressure
Duty cycle	0.5	Fraction of cycle time for chest compression
f_{tp}	0—1.0	Thoracic pump factor (0.75 = adult, 0.25 = child, 1.0 = emphysema, 0 = open chest)
Pinit	5 mmHg	Initial equilibrium pressure of arrested circulation
Fmax-chest	0—500 Nt	Maximum external force on sternum
x_0	0—4 cm	Effective compression threshold

2.4.4. Test cases and validation

The spreadsheet code was validated by solving simple test cases for very small or very large values of the resistances and compliances and by establishing a model of the normal adult circulation using normal right and left ventricular pressures with $f_{tp} = 0$. This model had an aortic blood pressure of 117/80 mmHg and a cardiac output of 5.1 L/min for a heart rate of 80/min, closely approximating the textbook normal values of 120/80 mmHg and 5.0 L/min.

2.5. Alternative definitions of perfusion pressure

In preliminary studies it became apparent that the precise mathematical definition of perfusion pressure had a substantial impact upon the results. Often in resuscitation research coronary perfusion pressure is used as a synonym for systemic perfusion pressure (SPP) to indicate the simple difference between thoracic aortic pressure and right atrial or central venous pressure. Indeed there is a substantial literature, including often cited work by Redding[35], Ralston[36], and Kern[34], to indicate that survival from experimental cardiac arrest is maximized when the difference between thoracic aortic and right atrial pressure is maximized. More precisely, it is the mean difference in coronary perfusion pressure that seems to determine resuscitation success.

In contrast to systemic perfusion, coronary perfusion depends upon two subtle aspects of anatomy and physiology. These are the presence of the Thebesian vessels and the special importance of tissue pressure in the ventricular walls. The Thebesian vessels are small veins that drain from the walls of the cardiac ventricles directly into the right and left ventricular chambers. That is, some of the venous return goes directly into the ventricular chambers, rather than into cardiac veins that drain into the coronary sinus and then into the right atrium. Such veins drain the inner one third of the left ventricular wall[37,38]. When left ventricular pressure is too high between heartbeats, the inner third of the ventricular wall does not get enough blood flow.

In addition increased intramyocardial wall pressure causes collapse of capillary blood vessels and can stop heart muscle perfusion, even if right atrial pressure and cardiac venous pressure is low. Cardiologists refer to this phenomenon as the "vascular waterfall"[39-43]. The metaphor is intended to convey the idea that the flow over a waterfall is related to the drop in height from an upstream point to the edge of the waterfall, rather than the drop in height from an upstream point to the bottom of the waterfall. This situation is akin to that in the brain, where cerebral perfusion pressure is the difference between cerebral artery pressure and either cerebral venous pressure OR intracranial pressure, whichever is higher.

During cardiac arrest and CPR the ventricular walls are subjected to both external and internal pressures. There is substantial pressure on the epicardial surface during chest compression, which does not occur in the normal state. Here we define ventricular wall pressure as the average of intracavitary pressure and mediastinal pressure. In turn coronary perfusion pressure (CPP) is defined in the present study as mean thoracic aortic pressure minus left ventricular wall pressure. Systemic perfusion pressure (SPP) is defined in the traditional way as thoracic aortic pressure minus right atrial pressure. For purposes of simulated evolution mean values of either SPP or CPP are taken as figures of merit (fitness) to indicate the quality of CPR.

3. Results

The entire study involved testing of 64,414 different waveforms, always forsaking less effective ones for more effective ones. The process generated 40 highly evolved waveform "genomes", each derived from a different random progenitor, after an average of 1610 generations. Twenty waveforms evolved to maximize SPP, and 20 waveforms evolved to maximize CPP. Six representative evolved waveforms are illustrated in Figures 5 and 6, together with the corresponding values of SPP or CPP. As is quite evident, the fundamental design concept discovered by simulated evolution is that of reciprocal pumping. That is, whenever the chest is being compressed, the abdomen is being decompressed, and vis versa. In addition, chest compression nearly always reached the maximal allowable level, as did chest decompression. Similarly, abdominal compression nearly always reached the maximal allowable level, as did abdominal decompression, spanning the full range of amplitude. Thus simulated evolution discovered the principles of active compression-decompression (ACD-) CPR and of interposed abdominal compression (IAC-) CPR. Interestingly, however, when SPP was maximized there tended to be relatively longer periods of chest compression and abdominal decompression. However, when CPP was maximized there tended to be relatively longer periods of abdominal compression and chest decompression.

The difference between seeking maximum SPP and seeking maximum CPP is reflected in mean values for the duty cycle of chest compression—namely the percentage of total cycle time spent in chest compression and abdominal decompression. For maximum SPP the duty cycles of chest compression ranged form 54 to 71 percent. The average duty cycle was 61 ± 7 percent. For maximum CPP the duty cycles of the chest compression ranged form 25 to 42 percent. The average duty cycle was 28 ± 5 percent. On average the 20 waveforms evolved to maximize SPP, produced a systemic perfusion pressure of 78 ± 4 mmHg and a forward flow of 4.7 L/min. The 20 waveforms evolved to optimize CPP, produced a coronary perfusion pressure of 40 mmHg and a forward flow of 3.4 L/min. To maximize coronary blood flow the time spent in chest compression was one half that required to maximize systemic blood flow. Just as in the case of the normal circulation, longer periods of diastole are congenial to coronary blood flow.

There were also differences in compression rate (the compression frequency or number of compression cycles per minute) between the two fitness criteria. For maximal SPP the compression rates of surviving waveforms ranged from 80 to 140 cycles/min. The average compression rate was 104 ± 23 cycles/min. For maximal CPP the compression rates of surviving waveforms ranged from 40 to 100 cycles/min. The average compression rate was 67 ± 21 cycles/min.

To determine if the idiosyncrasies and vagaries of particular evolved waveforms such as those in Figures 5 and 6 are functionally important, or merely evolutionary dead wood, it is useful to explore the performance of regular reciprocal pumping waveforms of constant frequency and duty cycle. Such hybrid waveforms embody the design features evolved to maximize perfusion pressures and yet are simple and practical to implement. For these waveforms compression and decompression are always reciprocal. One applies abdominal decompression whenever there is chest compression, and one applies abdominal compression whenever there is chest decompression. Figure 7 illustrates one example of such a hybrid compression waveform using rectangular waves—that is sharp transition between high and low pressure states, as tended to evolve in computer simulations.

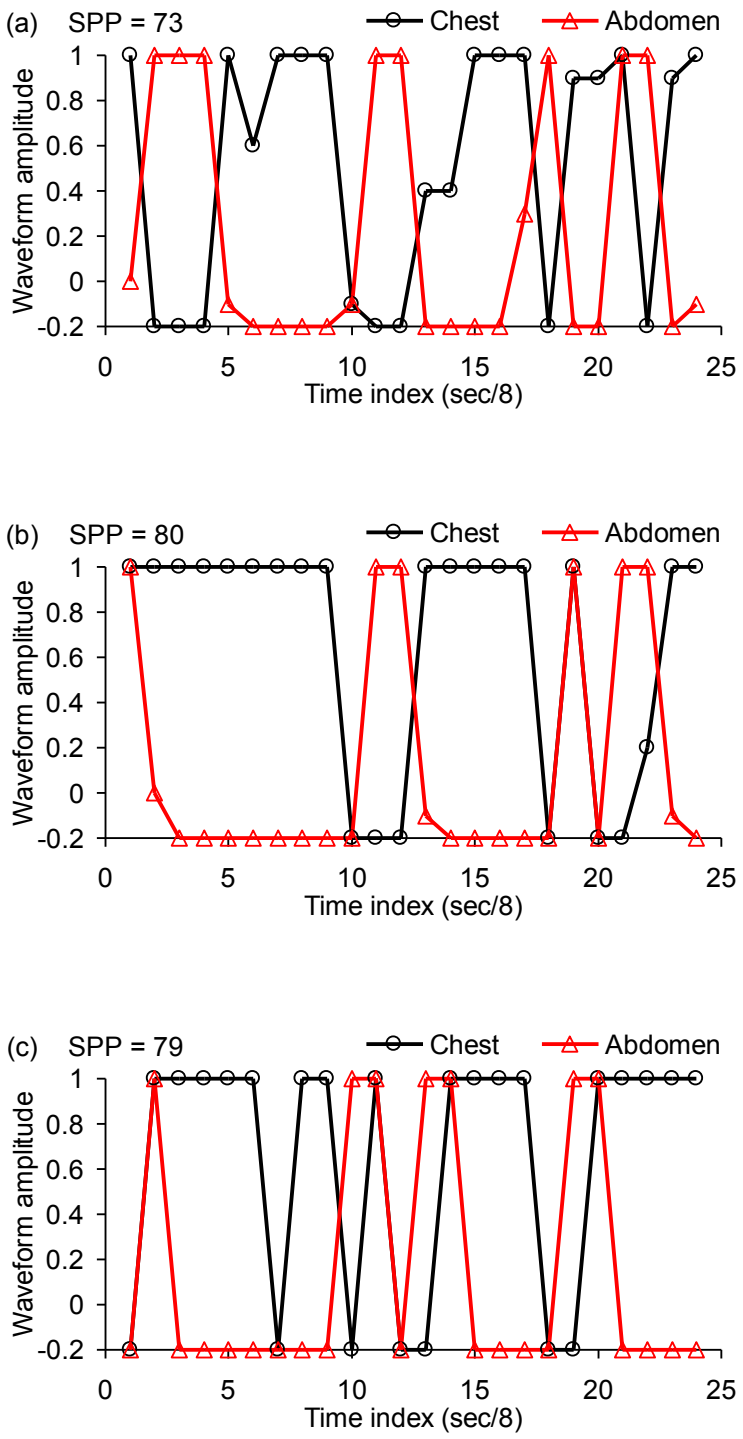

Figure 5. Highly evolved waveforms for chest and abdominal compression and decompression that maximize systemic perfusion pressure (SPP) in CPR. Three particular examples are shown. Thoracic pump factor 0.75. Maximal chest compression force 400 Nt. Maximal abdominal pressure 100 mmHg.

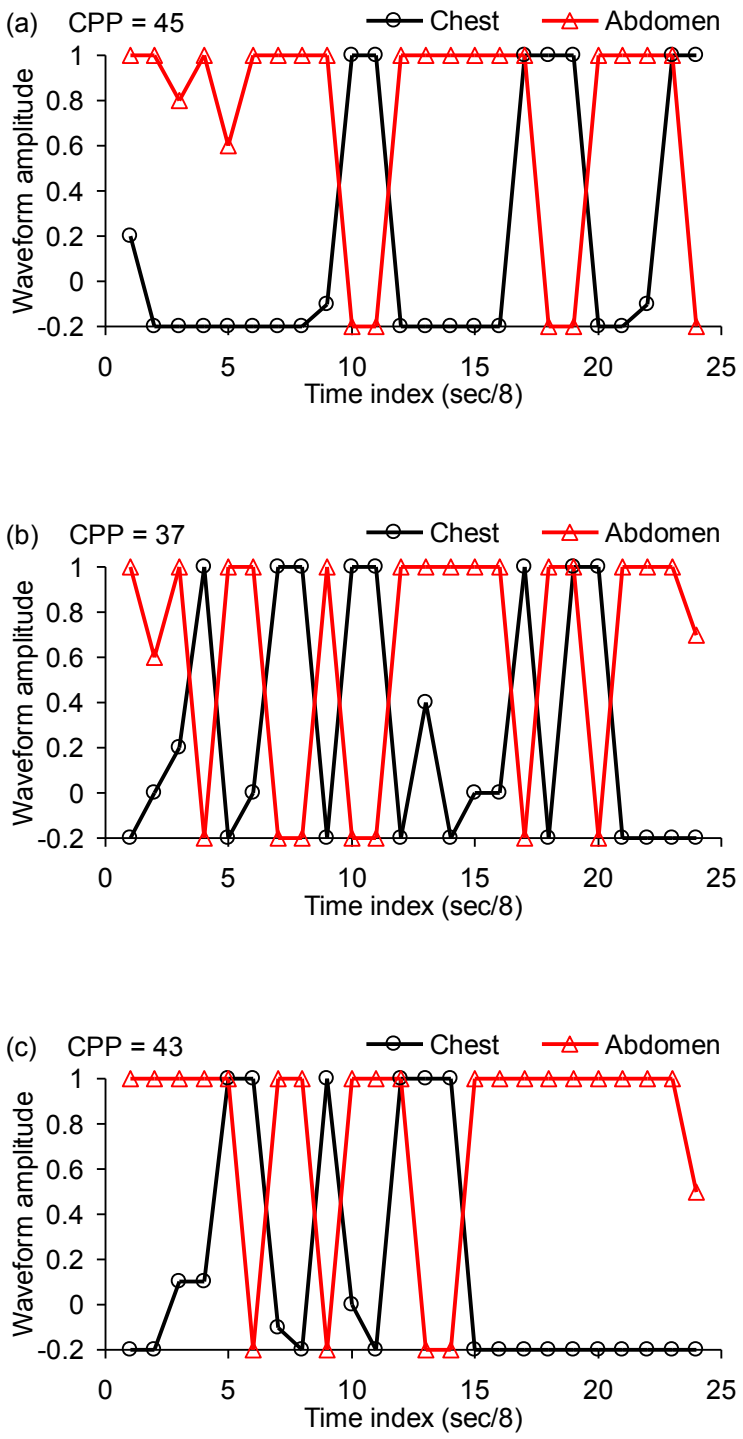

Figure 6. Highly evolved waveforms for chest and abdominal compression and decompression that maximize coronary perfusion pressure (CPP) in CPR. Three particular examples are shown. Thoracic pump factor 0.75. Maximal chest compression force 400 Nt. Maximal abdominal pressure 100 mmHg.

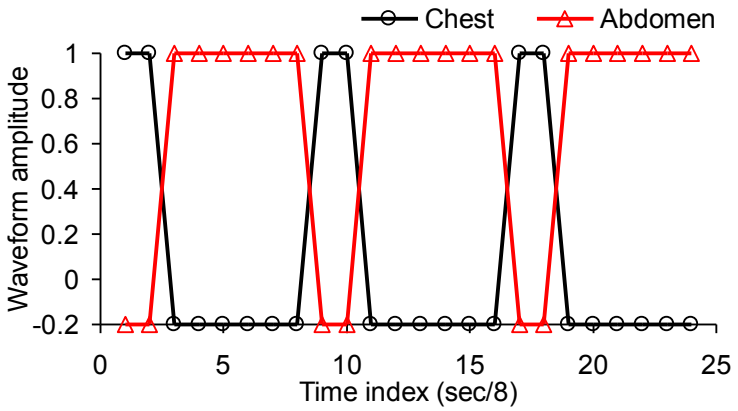

Figure 7. A regular reciprocal waveform for chest and abdominal compression and decompression. This example has a cycle rate of 60/min and a duty cycle for chest compression of 25 percent.

Figure 8 shows the SPP and CPP surfaces above the frequency-duty cycle plane for these regular waveforms. Each point on the surface represents perfusion pressure at a particular combination of compression frequency and duty cycle. In these simplified two dimensional search spaces the optimal parameters are easy to identify. The peak value of SPP (87 mmHg) and CPP (44 mmHg) generated by the regular waveforms are similar to those of the best-evolved waveforms (85 for SPP and 46 for CPP). Thus the irregularities in particular evolved waveforms are not critical for performance. To maximize SPP one needs a frequency near 60/min and a duty cycle of about 70 percent. To maximize CPP one needs a frequency of near 100/min and a duty cycle of about 30 percent. A compromise waveform worth noting is that having a frequency of 80/min and a duty cycle of 50 percent, which would produce near maximal systemic and coronary perfusion.

As shown in Figure 9, the compromise 4-phase 80/min, 50% waveform inspired by simulated evolution compares favorably to standard CPR and to various modified methods of CPR that have been developed in laboratory experiments. Here, to more realistically simulate manual chest and abdominal compression, a triangular pattern was used for each compression. That is, individual compressions of the chest and abdomen rise to a single peak value and then fall back to baseline decompression. In exactly the same test system the 4-phase 80/min, 50% waveform produces greater SPP and CPP than standard CPR, active compression-decompression CPR with an impedance threshold valve, and interposed abdominal compression CPR. Four-phase CPR with compression and decompression of both the chest and the abdomen at 80min and 50% duty cycle appears to add increased efficacy to external cardiopulmonary resuscitation.

Figure 10 shows time domain tracings of selected intrathoracic pressures during 4-phase 80/min, 50% duty cycle CPR as could be performed manually with a Life-stick like device. There is a substantial gap between aortic and right atrial pressures, providing systemic perfusion of 3.8 L/min at a mean systemic perfusion pressure of 61 mmHg. There is also a modest diastolic gap between aortic pressure and left ventricular intracavitary pressure, providing for myocardial perfusion. However, both pulmonary artery and left ventricular pressures are on average much higher than during the normal activity of a beating

heart. This observation raises the possibility of the rapid accumulation of pulmonary edema if CPR is maintained for long periods.

(a)

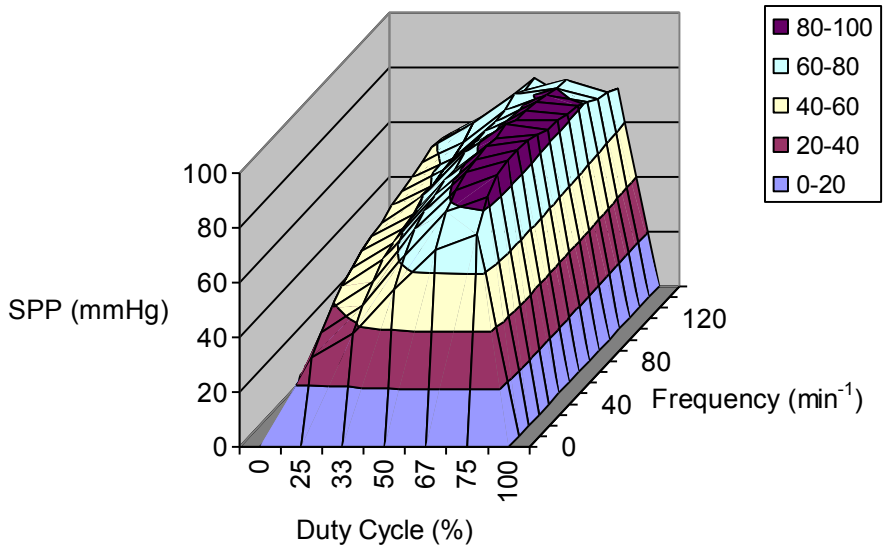

(b)

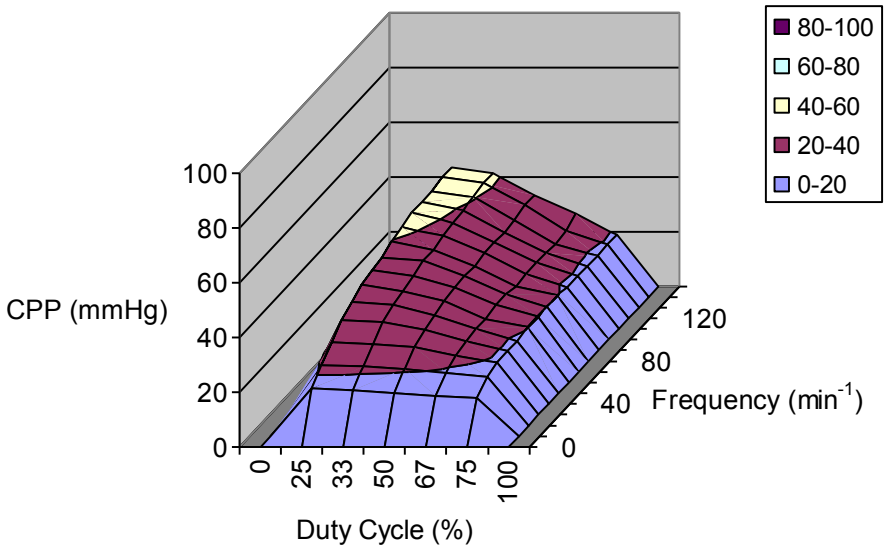

Figure 8. Mean perfusion pressure during simulated 4-phase CPR with regular waveforms at various compression frequencies and duty cycles. (a) systemic perfusion pressure SPP, (b) coronary perfusion pressure CPP. Perfusion pressures plotted are average, nearly steady-state, values during cycles 20 through 25 after onset of CPR.

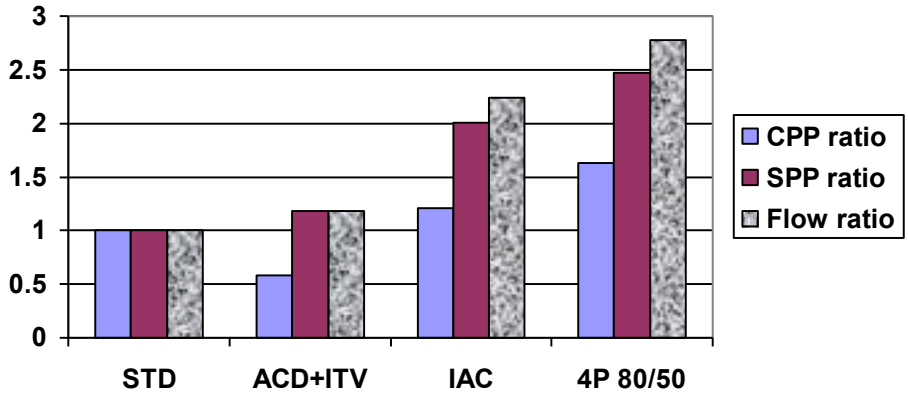

Figure 9. Ratios of perfusion pressures and systemic blood flow to those with standard CPR for alternative thoraco-abdominal compression techniques including standard CPR (STD), active compression-decompression CPR with an impedance threshold valve (ACD+ITV), interposed abdominal compression CPR (IAC), and 4-phase CPR at 80 cycles/min and 50% duty cycle (4P 80/50). Reference values (1.0) for STD CPR: CPP 13.1 mmHg; SPP 24.4 mmHg; flow 1.36 L/min.

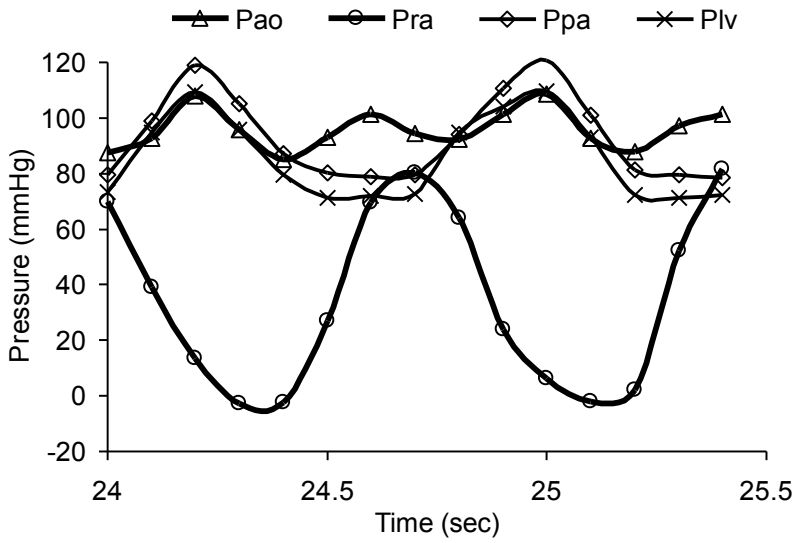

Figure 10. Multi-channel pressure tracings for 4-phase 80/min, 50% duty cycle CPR as could be performed manually with a Life-stick like device. For added realism individual compressions of chest and abdomen rise to a peak value and then fall to baseline in a triangular pattern in time. That is, sustained compression is not maintained as in the ideal, evolved waveforms. CPP = 19 mmHg, SPP = 61 mmHg, forward flow = 3.8 L/min.

4. Discussion

Given the extreme practical difficulties of working with human or animal models of cardiac arrest and CPR, computer models have found a niche in resuscitation research[44,45]. Although obviously lacking in blood-and-guts biology, such models are independent of many confounding factors present in laboratory studies and in clinical trials. These include varying patient populations, cardiac arrest time, drug therapy, underlying disease, chest configuration, and body size, as well as varying rescuer size, skill, strength, consistency, prior training, and bias. Computer models also allow precise comparisons of various techniques in exactly the same test system. It is not necessary to compare experiments in different animal models or clinical studies in different patient populations. The consistency and precision of computer models also makes simulated evolution possible. Even slight differences in the effectiveness of one technique over another can be detected and used to select improved techniques. This strategy would be impractical in clinical models, because of the very large numbers of patients required to establish the statistical significance of small improvements in outcome[46].

The strategy of simulated evolution in computer models can create a very large number of alternative hypotheses, combined with a brutal pruning mechanism to weed out less effective methods. Few laboratories have done such head-to-head comparisons, and few scientists are eager to abandon a pet idea, once discovered. Simulated evolution can do this with utter dispassion, thereby groping toward an optimal solution. Moreover, by using simulated evolution to search for design concepts rather than particular solutions, human investigators can short-circuit the process by many generations to arrive at a practical solution quickly. That is, a thoughtful scientist or engineer can make an intelligent guess as to the pristine design that evolution is groping towards. This is a sensible division of labor between man and machine, especially since any particular evolved waveform would have to be simplified anyway for use by human rescuers or even mechanical devices.

In some ways the simulated evolution reported here has recapitulated 50 years of CPR research. It found the design concepts of active compression—decompression CPR, interposed abdominal compression CPR, and the potential value of vest and/or Life-stick-like systems. Since none of the 40 random seed values evolved into a radically different waveform, we can have some confidence that resuscitation research has not missed an important big idea. The three dimensional plots of Figure 8 strongly resemble those published in 1981 by Fitzgerald[47] to describe the influence of compression rate and duty cycle on chest compression only CPR in dogs using an analytical approach that focused on pump filling and emptying times. The concept of maximizing perfusion of the myocardium with 30 percent duty cycle and perfusion of the brain with about 60 percent duty cycle was advanced by Babbs and Thelander[48] in 1995 for interposed abdominal compression CPR (no decompression) using a digital computer model of the circulation implemented in SPICE. Thus the results of simulated evolution nicely summarize and extend much earlier research into the question of how to generate more artificial circulation during cardiac arrest. It is now perhaps time to consolidate these concepts from a variety of research laboratories and clinics to create the next generation of techniques.

With new solutions come new problems. One special point of concern is the high pulmonary vascular pressures generated by the evolved waveforms. If sustained for many minutes to hours, such high pressures would surely lead to pulmonary edema. A clue to the magnitude of this phenomenon can be found by considering the high-pressure capillaries in the renal glomeruli. These normally receive a

blood flow of about 1 L/min (1/5 normal cardiac output) and produce a glomerular filtration rate of 100 ml/min. If total blood flow in 4-phase CPR were to approach 4 L/min, then the rate of pulmonary edema formation could approach 400 ml/min. This value might be tolerable for several minutes when compared to a total lung volume for an adult human of about 7 liters. However, with continuing high pressure CPR, pulmonary flooding could be a problem. Such pulmonary flooding might be counteracted by some form of high pressure ventilation[49], especially if applied in a way that did not compromise coronary perfusion.

There is more to evolution than what is presented here. Robustness to environmental change is another desirable feature of evolved organisms. In the context of the present problem, this could mean subjecting evolved waveforms to random variations in chest compression technique, variable pauses for ventilation, simulated vasopressor effects, spontaneous changes in vascular resistance and compliance during prolonged cardiac arrest, simulated broken ribs, etc. Maximal parsimony can be included in evolution by adding a penalty for complexity. Adaptive features and the ability to learn are also popular research topics in simulated evolution[14]. If sensors were available for variables such as end tidal CO_2 concentration to provide feedback, and if the evolving forms could use information from the sensors to fine-tune their responses, then a whole new generation of actively controlled techniques might emerge.

Conclusion

Simulated evolution in the present study began with no constraints other than maximal and minimal pressures, which are related to safety and practicality, and the constraint of periodicity. Within this universe, discretized into 13 compression/decompression levels and 24 time steps per period there are $13^{24} \sim 5 \times 10^{26}$ possible chest compression waveforms, each of which could be paired with an equal number of possible abdominal compression waveforms, giving 25×10^{52} possibilities. The process of simulated evolution was conducted with mathematical dispassion and could have converged to any available solutions. Yet it seemed to recapitulate 50 years of resuscitation research in about two days of total computing time on a Pentium III machine. Simulated evolution discovered the principles of interposed abdominal compression CPR[3,7,50] and of active compression-decompression CPR[51,52]. If one chooses to optimize coronary perfusion pressure at shorter duty cycles and rates over 80/min, then evolution also discovered high impulse CPR[53,54]. The present results suggest that it might be better to quit arguing about which of these known approaches is better and to focus instead on combining them for best results. With combined chest and abdominal compression and decompression it may be possible to achieve artificial circulation approaching normal resting cardiac output in adults. Although problems such as pulmonary edema may need to be dealt with, given the current dismal outcome from sudden cardiac death, such problems would be a refreshing change. It is time to move beyond endless calls for more research and to implement more effective external compression waveforms.

References

1. Sack JB, Kesselbrenner MB, Bregman D. Survival from in-hospital cardiac arrest with interposed abdominal counterpulsation during cardiopulmonary resuscitation. JAMA 1992;267:379-85.
2. Sack JB, Kesselbrenner MB. Hemodynamics, survival benefits, and complications of interposed abdominal compression during cardiopulmonary resuscitation. Acad Emerg Med 1994;1:490-7.
3. Babbs CF, Sack JB, Kern KB. Interposed abdominal compression as an adjunct to cardiopulmonary resuscitation. American heart journal 1994;127:412-21.
4. Aufderheide TP, Pirrallo RG, Provo TA, Lurie KG. Clinical evaluation of an inspiratory impedance threshold device during standard cardiopulmonary resuscitation. Circulation 2004;110 (Suppl III):III-413.
5. Pirrallo RG, Aufderheide TP, Provo TA, Lurie KG. An impedance threshold device significantly increases invasively measured arterial pressures during standard cardiopulmonary resuscitation in out-of-hospital cardiac arrest. Circulation 2004;110 (Suppl III):III-414.
6. Thayne RC, vanDellen A, Thomas DC, Neville JD. An impedance threshold device improves short-term outcomes following out-of-hospital cardiac arrest. Circulation 2004;110 (Suppl III):III-414-15.
7. Babbs CF. Interposed abdominal compression CPR: a comprehensive evidence based review. Resuscitation 2003;59:71-82.
8. Plaisance P, Lurie KG, Vicaut E, et al. A comparison of standard cardiopulmonary resuscitation and active compression-decompression resuscitation for out-of-hospital cardiac arrest. French Active Compression-Decompression Cardiopulmonary Resuscitation Study Group. N Engl J Med 1999;341:569-75.
9. Lurie KG. Recent advances in mechanical methods of cardiopulmonary resuscitation. Acta Anaesthesiol Scand Suppl 1997;111:49-52.
10. Beattie C, Guerci AD, Hall T, et al. Mechanisms of blood flow during pneumatic vest cardiopulmonary resuscitation. J Appl Physiol 1991;70:454-65.
11. Tang W, Weil MH, Schock RB, et al. Phased chest and abdominal compression-decompression. A new option for cardiopulmonary resuscitation. Circulation 1997;95:1335-40.
12. Back T, Schwefel H-P. An overview of evolutionary algorithms for parameter optimization. Evolutionary Computation 1993;1:1-23.
13. Back T. Evolutionary Algorithms in Theory and Practice. 1 ed. Oxford: Oxford University Press; 1996.
14. Parmee IC. Evolutionary and Adaptive Computing in Engineering Design. London: Springer; 2001.
15. Fogel LJ, Owens AJ, Walsh MJ. Artificial Intelligence Through Simulated Evolution. New York: John Wiley & Sons, Inc.; 1966.
16. Babbs CF, Thelander K. Theoretically optimal duty cycles for chest and abdominal compression during external cardiopulmonary resuscitation [see comments]. Acad Emerg Med 1995;2:698-707.
17. Babbs CF, Weaver JC, Ralston SH, Geddes LA. Cardiac, thoracic, and abdominal pump mechanisms in CPR: studies in an electrical model of the circulation. American Journal of Emergency Medicine 1984;2:299-308.

18. Babbs CF. CPR techniques that combine chest and abdominal compression and decompression: Hemodynamic insights from a spreadsheet model. Circulation 1999;100:2146-52.
19. Shultz JJ, Coffeen P, Sweeney M, et al. Evaluation of standard and active compression-decompression CPR in an acute human model of ventricular fibrillation. Circulation 1994;89:684-93.
20. Carli PA, De La Coussaye JE, Riou B, Sassine A, Eledjam JJ. Ventilatory effects of active compression-decompression in dogs. Ann Emerg Med 1994;24:890-4.
21. Babbs CF. Effects of an impedance threshold valve upon hemodynamics in standard CPR: studies in a refined computational model. Resuscitation 2005;66:335-45.
22. Niemann JT, Ung S, Rosborough JP, Suzuki J, Criley JM. Preferential brachiocephalic flow during CPR--a hemodynamic explanation. Circulation 64(IV) 1981:303.
23. Gruben KG, Guerci AD, Popel AS, Tsitlik JE. Sternal force-displacement relationship during cardiopulmonary resuscitation. Journal of Biomechanical Engineering 1993;115:195-201.
24. Rudikoff MT, Maughan WL, Effron M, Freund P, Weisfeldt ML. Mechanisms of blood flow during cardiopulmonary resuscitation. Circulation 1980;61:345-52.
25. Weiser FM, Adler LN, Kuhn LA. Hemodynamic effects of closed and open chest cardiac resuscitation in normal dogs and those with acute myocardial infarction. In: Am J Cardiol; 1962; 1962. p. 555-61.
26. Sanders AB, Kern KB, Ewy GA, Atlas M, Bailey L. Improved resuscitation from cardiac arrest with open chest massage. In: Annal Emerg Med 13; 1984; 1984. p. 672-5.
27. Babbs CF. Hemodynamic mechanisms in CPR: a theoretical rationale for resuscitative thoracotomy in non-traumatic cardiac arrest. Resuscitation 1987;15:37-50.
28. Paradis NA, Martin GB, Goetting MG, et al. Simultaneous aortic, jugular bulb, and right atrial pressures during cardiopulmonary resuscitation in humans: Insights into mechanisms. Circulation 1989;80:361-8.
29. Halperin HR, Tsitlik JE, Guerci AD, et al. Determinants of blood flow to vital organs during cardiopulmonary resuscitation in dogs. Circulation 1986;73:539-50.
30. Chandra NC. Mechanisms of blood flow during CPR. Ann Emerg Med 1993;22:281-8.
31. Babbs CF, Voorhees WD, Fitzgerald KR, Holmes HR, Geddes LA. Relationship of artificial cardiac output to chest compression amplitude--evidence for an effective compression threshold. Annals of Emergency Medicine 1983;12:527-32.
32. Babbs CF, Weaver JC, Ralston SH, Geddes LA. Cardiac, thoracic, and abdominal pump mechanisms in cardiopulmonary resuscitation: studies in an electrical model of the circulation. Am J Emerg Med 1984;2:299-308.
33. Babbs CF, Ralston SH, Geddes LA. Theoretical advantages of abdominal counterpulsation in CPR as demonstrated in a simple electrical model of the circulation. Annals of Emergency Medicine 1984;13:660-71.
34. Kern KB, Ewy GA, Voorhees WD, Babbs CF, Tacker WA. Myocardial perfusion pressure: a predictor of 24-hour survival during prolonged cardiac arrest in dogs. Resuscitation 1988;16:241-50.
35. Redding JS. Abdominal compression in cardiopulmonary resuscitation. Anesthesia and Analgesia 1971;50:668-75.
36. Ralston SH, Voorhees WD, Babbs CF. Intrapulmonary epinephrine during cardiopulmonary resuscitation: Improved regional blood flow and resuscitation in dogs. Annals of Emergency Medicine 1984;13:79-86.

37. Taylor JR, Taylor AJ. Thebesian sinusoids: forgotten collaterals to papillary muscles. Can J Cardiol 2000;16:1391-7.
38. Nordenstrom B. The Thebesian circulation in coronary angiography. Angiology 1965;16:616-21.
39. Downey JM, Kirk ES. Inhibition of coronary blood flow by a vascular waterfall mechanism. Circ Res 1975;36:753-60.
40. Westerhof N, Sipkema P, Van Huis GA. Coronary pressure-flow relations and the vascular waterfall. Cardiovasc Res 1983;17:162-9.
41. Jan KM. Distribution of myocardial stress and its influence on coronary blood flow. J Biomech 1985;18:815-20.
42. Gosselin RE, Kaplow SM. Venous waterfalls in coronary circulation. J Theor Biol 1991;149:265-79.
43. Farhi ER, Klocke FJ, Mates RE, et al. Tone-dependent waterfall behavior during venous pressure elevation in isolated canine hearts. Circ Res 1991;68:392-401.
44. Babbs CF. Circulatory adjuncts. Newer methods of cardiopulmonary resuscitation. Cardiol Clin 2002;20:37-59.
45. Christenson JM. Cardiopulmonary resuscitation research models: motherboards, mammals, and man. Acad Emerg Med 1995;2:669-71.
46. Babbs CF. Consensus evidence evaluation in resuscitation research: analysis of Type I and Type II errors. Resuscitation 2001;51:193-205.
47. Fitzgerald KR, Babbs CF, Frissora HA, Davis RW, Silver DI. Cardiac output during cardiopulmonary resuscitation at various compression rates and durations. American Journal of Physiology 1981;241:H442-H8.
48. Babbs CF, Thelander K. Theoretically optimal duty cycles for chest and abdominal compression during external cardiopulmonary resuscitation. Acad Emerg Med 1995;2:698-707.
49. Voelckel WG, Lurie KG, Zielinski T, et al. The effects of positive end-expiratory pressure during active compression decompression cardiopulmonary resuscitation with the inspiratory threshold valve. Anesth Analg 2001;92:967-74.
50. Babbs CF, Tacker WA. Cardiopulmonary resuscitation with interposed abdominal compression. Circulation 1986;74(suppl IV):37-41.
51. Lurie KG. Active compression-decompression CPR: a progress report. Resuscitation 1994;28:115-22.
52. Lurie KG, Coffeen P, Shultz J, McKnite S, Detloff B, Mulligan K. Improving active compression-decompression cardiopulmonary resuscitation with an inspiratory impedance valve. Circulation 1995;91:1629-32.
53. Maier GW, Tyson GS, Olsen CO, et al. The physiology of external cardiac massage: high-impulse cardiopulmonary resuscitation. Circulation 1984;70:86-101.
54. Maier GW, Newton JR, Wolfe JA, et al. The influence of manual chest compression rate on hemodynamic support during cardiac arrest: high-impulse cardiopulmonary resuscitation. Circulation 1986;74(Suppl IV):IV-51-9.
55. Brekhovskikh LM, Goncharov V. Mechanics of Continua and Wave Dynamics. Second ed. Berlin: Springer-Verlag; 1994.
56. Fung YC. Biomechanics : mechanical properties of living tissues. New York: Springer-Verlag; 1981.
57. DelGuercio L, Feins NR, Cohn JD, Coomaraswamy RP, Wollman SB, State D. Comparison of blood flow during external and internal cardiac massage in man. In: Circulation 31(Suppl I); 1965; 1965. p. 171-80.

58. Goyal RK, Biancani P, Phillips A, Spiro HM. Mechanical properties of the esophageal wall. J Clin Invest 1971;50:1456-65.
59. Takeda T, Kassab G, Liu J, Puckett JL, Mittal RR, Mittal RK. A novel ultrasound technique to study the biomechanics of the human esophagus in vivo. Am J Physiol Gastrointest Liver Physiol 2002;282:G785-93.
60. Fan Y, Gregersen H, Kassab GS. A two-layered mechanical model of the rat esophagus. Experiment and theory. Biomed Eng Online 2004;3:40.
61. Matthews FL, West JB. Finite element displacement analysis of a lung. J Biomech 1972;5:591-600.
62. Hoppin FG, Jr., Lee GC, Dawson SV. Properties of lung parenchyma in distortion. J Appl Physiol 1975;39:742-51.
63. Lai-Fook SJ, Wilson TA, Hyatt RE, Rodarte JR. Elastic constants of inflated lobes of dog lungs. J Appl Physiol 1976;40:508-13.
64. Karakaplan AD, Bieniek MP, Skalak R. A mathematical model of lung parenchyma. J Biomech Eng 1980;102:124-36.
65. Barbenel JC, Evans JH, Finlay JB. Stress-strain-time relations for soft connective tissuese. In: Kenedi RM, ed. Perspectives in Biomedical Engineering. Baltimore: University Park Press; 1973:165-72.
66. Tong P, Fung YC. The stress-strain relationship for the skin. J Biomech 1976;9:649-57.
67. Chu BM, Frasher WG, Wayland H. Hysteretic behavior of soft living animal tissue. Ann Biomed Eng 1972;1:182-203.
68. Patel DJ, Schilder DP, Mallos AJ. Mechanical properties and dimensions of the major pulmonary arteries. J Appl Physiol 1960;15:92-6.
69. Hamilton(Section-Editor) WF, Dow(Executive-Editor) P. Handbook of Physiology Volume 2, Section 2: Circulation: American Physiological Society, Washington D.C.; 1963.
70. Antoni H. Functional Properties of the Heart. In: Greger R, ed. Comprehensive Human Physiology. Berlin, Heidelberg: Springer-Verlag; 1996:1801-23.

Appendix: computational model of the circulatory system

Variable are defined in Table 1. Standard values of parameters are provided in Table 2.

A1.1. Depth of chest compression

Motion of the sternum in response to force F(t) is given by the differential equation

$$F(t) - kx_1 - \mu\dot{x}_1 = 0, \qquad (1)$$

for sternal displacement, x_1, and velocity of displacement $\dot{x}_1$. This simple spring and damper model reproduces the experimentally measured force displacement data for the human chest[23], including hysteresis. For numerical computation it is sufficient to specify the velocity of the sternum as $\dot{x}_1 = (F(t) - kx_1)/\mu$, keeping track of the sternal position as a function of time, t, as $x_1 = \int_0^t \dot{x}_1 dt$.

A1.2. Mediastinal pressure

Pressure on the heart and great vessels impels circulation in CPR. Let us denote the mediastinal pressure caused by chest compression as P_M. For simplicity let us regard the mediastinum as an elastic material for which internal stress (pressure) is related to the strain (percent compression) by a constant known as Young's modulus of elasticity, E. In particular, the pressure is equal to Young's modulus of elasticity, E, multiplied by the strain[55]. Let x_2 represent the anteroposterior expansion of the heart due to changes in its internal blood volume. Then the pressure on the outer surface of the heart is

$$P_M = E(x_1 + x_2)/d_0, \qquad (2a)$$

and the time rate of change in external pressure on the heart is

$$\dot{P}_M = E(\dot{x}_1 + \dot{x}_2)/d_0. \qquad (2b)$$

We can solve Eq. (1) for $\dot{x}_1 = (F(t) - kx_1)/\mu$, knowing the force on the chest as a function of time, and constants k and μ. We can also know the rate of expansion, $\dot{x}_2$, based upon the average cross sectional area of the heart chamber (~20 cm^2), which can be estimated from anatomy, and the inflow and outflow rates for the heart chamber, which will be known from operation of the rest of the circulatory model. In this case $\dot{x}_2 = (i_{in} - i_{out})/A_c$, where i_{in} is the rate of inflow into the cardiac chamber, i_{out} is the rate of outflow, and A_c is the characteristic cross sectional area of the chamber. The key idea is that when a particular cardiac chamber fills with blood, it encroaches on precardiac and retrocardiac tissue. The opposite effect happens when the chamber empties.

Young's modulus of elasticity for pericardiac tissues can be estimated from published biomechanical studies of the elastic properties of lung, esophagus, and loose connective tissue (Table 3). For small

strains in the neighborhood of 10 to 30 percent, E can be considered constant[56]. Taking an average value of the soft tissues from Table 3, as E ~ 12,000 Pa, estimating d_0 for combined precardiac and retrocardiac tissues as 10 cm, noting 133 Pa = 1 mmHg, and substituting into Eq. 2, we can compute the external pressure on the heart in mmHg as

$$P_M \approx \frac{12000}{1330}(x_1 + x_2) \approx 9(x_1 + x_2)\ \text{mmHg}, \text{ and} \qquad (3a)$$

$$\dot{P}_M \approx 9(\dot{x}_1 + \dot{x}_2)\ \text{mmHg/sec}. \qquad (3b)$$

This relationship is rather credible on the basis of animal and human studies of CPR in which intrathoracic pressures have been measured in the cardiac chambers and the esophagus[28,31,57]. On the basis of these studies one can estimate that a 5 cm sternal depression produces a roughly 50 mmHg increase in intrathoracic pressure, which would suggest that $P_M(x) \approx 10\, x_1$ for x_1 in cm and $P_M(x_1)$ in mmHg, which is remarkably close to (3a).

Table 3 (Appendix 1): Elastic moduli of soft tissues.

Tissue	Approx. E (kPa)	Investigator	Year	Reference
Esophagus	15	Goyal	1971	[58]
Esophagus	15	Takeda	2002	[59]
Esophagus	25	Fan	2004	[60]
Lung	4	Matthews	1972	[61]
Lung	5	Hoppin	1975	[62]
Lung	1	Lai-Fook	1976	[63]
Lung	1	Karakaplan	1980	[64]
Skin	2	Barbenel	1973	[65]
Skin	22	Tong	1976	[66]
Mesentery	37	Chu	1972	[67]
Pulmonary artery	6	Patel	1960	[68]
Mean value	12			

A1.3. Lung pressure

From a mechanical viewpoint the lungs can be regarded as gas filled balloons open to air via the tracheobronchial tree. For these compartments the pressure compared to atmospheric pressure is $P_{lung} = (\Delta V_{chest} + V_{in} - V_{out})/C_{lung}$, where ΔV_{chest} is the decrease in lung volume do to chest compression in CPR, $V_{in} - V_{out}$ is the net volume added via the airways, and C_{lung} is the combined lung-chest wall compliance. Here for simplicity we do not include the net volume of blood leaving the thorax during chest compression (~20 ml), which is small compared to the lung volume change caused by chest compression (~500 ml).

The change in lung pressure over small time interval dt may be given by the expression

$$dP_{lung} = \frac{dt}{C_{lung}}\left[\dot{x}_1 A_L - \frac{\left(P_{lung} - P_{mouth}\right)}{R_{airway}}\right]. \qquad (4)$$

Here $\dot{x}_1$ is the rate of sternal compression, A_L is the cross sectional area of lung influenced by chest compression (~100 cm^2), and the left hand term, $\dot{x}_1 A_L$, is the volume swept out by chest compression. The right hand term is the flow out of the chest via the airways through airway resistance. The difference multiplied by dt is the volume change of uncompressed lung, which when divided by lung-chest compliance, gives the corresponding pressure change, assuming that the volume change is small with respect to total lung volume.

A1.4. Physiological parameters

Parameters describing a textbook normal "70 Kg man"[69] are used to specify values of the compliances and resistances in Figures 2 and 3. The normal 30-fold ratio of venous to arterial compliance characterizes a circulation in the absence of fluid loading or congestive heart failure. The distribution of vascular conductances (1/Resistances) into cranial, thoracic, and caudal components reflects textbook distributions of cardiac output to various body regions. Details of the rationale for selection of resistance and compliance values are provided in references[32,33,69]. The normal diastolic compliance of the left ventricle was taken from Greger and Windhorst's comprehensive textbook of physiology[70]. The diastolic compliance of the right ventricle was estimated as twice that of the left ventricle. The compliances pulmonary arteries and pulmonary veins are divided into central and peripheral compartments with compliances of peripheral compartments of pulmonary vessels one tenth those of the corresponding central compartments.

A1.5. Solving for circulatory pressures

The relationships among the pressures in the various vascular compartments are determined by the definition of compliance and by Ohm's Law. The definition of compliance is $C = \Delta V / \Delta P$, where C is compliance, and ΔP is the incremental change in pressure within a compartment as volume ΔV is introduced. Ohm's Law, which relates flow to pressure and resistance, is $i = (P_1 - P_2)/R$, where

$P_1 - P_2$ is the instantaneous difference in pressure across resistance R as flow i occurs. In Figure 2 currents i_c (carotid), i_a (aortic), i_s (systemic), i_v (venous), i_j (jugular), i_{ia} (iliac artery), i_l (legs), i_{iv} (iliac veins), i_i (pump input), and i_o (pump output) are shown for clarity, with positive directions specified by arrows. In Figure 3 flows across each heart valve and the pulmonary vascular resistance are shown.

A1.4.1. Systemic vascular components

Applying these basic concepts with reference to Figures 2 and 3 provides a set of governing finite difference equations that can be used to describe hemodynamics. These equations are integrated numerically to describe instantaneous pressure vs. time waveforms in each compartment. Beginning, for example, with the abdominal aorta

$$\Delta V_{aa} = (i_a - i_s - i_{ia})\Delta t = \left[\frac{P_{ao} - P_{aa}}{R_a} - \frac{P_{aa} - P_{ivc}}{R_s} - \frac{P_{aa} - P_{fa}}{R_{ia}} \right] \Delta t \text{ , and}$$

$$\Delta P_{aa} = \Delta V_{aa} / C_{aa} . \qquad (5)$$

The term ΔV_{aa} represents the increase in abdominal aortic volume caused by net inflow of blood during the small time interval Δt. Substitution for currents, i_a , i_s , and i_{ia}, using Ohm's Law allows calculation of ΔV_{aa} from prevailing pressures.

Similarly, the pressure changes in other systemic vascular compartments are given by expressions (6) through (10), as follows.

$$\Delta V_{ivc} = (i_s - i_v + i_{fv})\Delta t = \left[\frac{P_{aa} - P_{ivc}}{R_s} - \frac{P_{ivc} - P_{ra}}{R_v} + \max\left(0 , \frac{P_{fv} - P_{ivc}}{R_{iv}} \right) \right] \Delta t$$

and

$$\Delta P_{ivc} = \Delta V_{ivc} / C_{ivc} . \qquad (6)$$

In (6) the max() function is used to represent the action of venous valves in the femoral and iliac veins that prevent retrograde flow. Similarly,

$$\Delta P_{car} = \frac{1}{C_{car}} (i_c - i_h)\Delta t = \frac{\Delta t}{C_{car}} \left[\frac{P_{ao} - P_{car}}{R_c} - \frac{P_{car} - P_{jug}}{R_h} \right] \qquad (7)$$

$$\Delta P_{jug} = \frac{1}{C_{jug}} (i_h - i_j)\Delta t = \frac{\Delta t}{C_{jug}} \left[\frac{P_{car} - P_{jug}}{R_h} - \max\left(0 , \frac{P_{jug} - P_{ra}}{R_j} \right) \right], \qquad (8)$$

where the max() function is used in expression (8) to implement the one-way valve action of Niemann's valves during cough or intrathoracic pressure pulses (when $P_{ra} > P_{jug}$).

The legs are represented as follows.

$$\Delta P_{fa} = \frac{1}{C_{fa}}(i_{ia} - i_l)\Delta t = \frac{\Delta t}{C_{fa}}\left[\frac{P_{aa} - P_{fa}}{R_{ia}} - \frac{P_{fa} - P_{fv}}{R_l}\right] \tag{9}$$

$$\Delta P_{fv} = \frac{1}{C_{fv}}(i_l - i_{fv})\Delta t = \frac{\Delta t}{C_{fv}}\left[\frac{P_{fa} - P_{fv}}{R_l} - \max\left(0\,,\,\frac{P_{fv} - P_{ivc}}{R_{iv}}\right)\right]. \tag{10}$$

For the peripheral pulmonary arteries

$$\Delta P_{ppa} = \Delta P_{lung} + \frac{\Delta t}{C_{ppa}}(i_3 - i_4) = \Delta P_{lung} + \frac{\Delta t}{C_{ppa}}\left[\frac{P_{pa} - P_{ppa}}{R_{cppa}} - \frac{P_{ppa} - P_{ppv}}{R_{pc}}\right]. \tag{11}$$

For the peripheral pulmonary veins

$$\Delta P_{ppv} = \Delta P_{lung} + \frac{\Delta t}{C_{ppv}}(i_4 - i_5) = \Delta P_{lung} + \frac{\Delta t}{C_{ppv}}\left[\frac{P_{ppa} - P_{ppv}}{R_{pc}} - \frac{P_{ppv} - P_{la}}{R_{cppv}}\right]. \tag{12}$$

A1.4.2. Chest pump components

For the thoracic aorta

$$\Delta V_{ao} = (i_o - i_c - i_a - i_{ht})\Delta t = \left[\max\left(0\,,\,\frac{P_{lv} - P_{ao}}{R_{av}}\right) - \frac{P_{ao} - P_{car}}{R_c} - \frac{P_{ao} - P_{aa}}{R_a} - \frac{P_{ao} - P_{ra}}{R_{ht}}\right]\Delta t$$

and

$$\Delta P_{ao} = \Delta P_{lung} + \frac{\Delta V_{ao}}{C_{ao}} + f_{tp}\frac{E}{d_0}\dot{x}_1\Delta t\ , \tag{13}$$

where f_{tp} is the thoracic pump factor. The rate of change in the diameter of the thoracic aorta is negligible with respect to $\dot{x}_1$ and so is omitted from Eq. 13.

For the central pulmonary arteries

$$\Delta V_{pa} = (i_2 - i_3)\Delta t = \left[\max\left(0\,,\,\frac{P_{rv} - P_{pa}}{R_{pv}}\right) - \frac{P_{pa} - P_{ppa}}{R_{cppa}}\right]\Delta t\ ,\ \text{and}$$

$$\Delta P_{pa} = \Delta P_{lung} + \frac{\Delta V_{pa}}{C_{pa}} + f_{tp}\frac{E}{d_0}\dot{x}_1\Delta t \qquad (14)$$

Corresponding expressions for the four chambers of the heart including the right and left ventricles and the right and left atria with their associated large veins (superior vena cava and central pulmonary veins) are computed from the sum of the mediastinal pressure and lung pressure acting on the chambers and the change in internal volume divided by chamber compliance. For these large, valved cardiac chambers $i_{in} \neq i_{out}$, and therefore $\dot{x}_2$ is not negligible.

Thus for the superior vena cava and right atrium

$$\Delta V_{ra} = (i_j + i_v + i_{ht} - i_i)\Delta t$$

$$= \left[\max\left(0, \frac{P_{jug} - P_{ra}}{R_j}\right) + \frac{P_{ivc} - P_{ra}}{R_v} + \frac{P_{ao} - P_{ra}}{R_{ht}} - \max\left(0, \frac{P_{ra} - P_{rv}}{R_{tv}}\right)\right]\Delta t,$$

where the max() functions indicate the actions of Niemann's valves and the tricuspid valve. In turn,

$$\Delta P_{ra} = \Delta P_{lung} + \frac{\Delta V_{ra}}{C_{ra}} + f_{tp}\frac{E}{d_0}\left(\dot{x}_1\Delta t + \frac{\Delta V_{ra}}{A_{ra}}\right). \qquad (15)$$

For the right ventricle

$$\Delta V_{rv} = (i_i - i_2)\Delta t = \left[\max\left(0, \frac{P_{ra} - P_{rv}}{R_{tv}}\right) - \max\left(0, \frac{P_{rv} - P_{pa}}{R_{pv}}\right)\right]\Delta t,$$

and

$$\Delta P_{rv} = \Delta P_{lung} + \frac{\Delta V_{rv}}{C_{rv}} + \frac{E}{d_0}\left(\dot{x}_1\Delta t + \frac{\Delta V_{rv}}{A_{rv}}\right). \qquad (16)$$

For the left atrium and central pulmonary veins

$$\Delta V_{la} = \left[\frac{P_{ppv} - P_{la}}{R_{cppv}} - \max\left(0, \frac{P_{la} - P_{lv}}{R_{mv}}\right)\right]\Delta t,$$

$$\Delta P_{la} = \Delta P_{lung} + \frac{\Delta V_{la}}{C_{la}} + f_{tp}\frac{E}{d_0}\left(\dot{x}_1\Delta t + \frac{\Delta V_{la}}{A_{la}}\right). \qquad (17)$$

Finally, for the left ventricle

$$\Delta V_{lv} = (i_6 - i_o)\Delta t = \left[\max\left(0, \frac{P_{la} - P_{lv}}{R_{mv}}\right) - \max\left(0, \frac{P_{lv} - P_{ao}}{R_{av}}\right) \right] \Delta t ,$$

$$\Delta P_{lv} = \Delta P_{lung} + \frac{\Delta V_{lv}}{C_{lv}} + \frac{E}{d_0}\left(\dot{x}_1 \Delta t + \frac{\Delta V_{lv}}{A_{lv}}\right). \qquad (18)$$